

**Bodyplan diversification in crinoid-associated myzostomes (Myzostomida, Protostomia)**Déborah Lanterbecq,^{1,a} Greg W. Rouse,² and Igor Eeckhaut¹¹ Marine Biology Laboratory, University of Mons-Hainaut, 7000 Mons, Hainaut, Belgium² Scripps Institution of Oceanography, University of California, San Diego,
La Jolla, California 92093-0202, USA

Abstract. When free-living organisms evolve into symbiotic organisms (parasites, commensals, or mutualists), their bodyplan is often dramatically modified as a consequence. The present work pertains to the study of this process in a group of marine obligate symbiotic worms, the Myzostomida. These are mainly ectocommensals and are only associated with echinoderms, mostly crinoids. Their usual textbook status as a class of the Annelida is generally accepted, although recent molecular phylogenetic studies have raised doubts on their relationships with other metazoans, and the question of their status remains open. Here, we reconstruct the evolution of their bodyplans by mapping 14 external morphological characters (analyzed using scanning electron microscopy) onto molecular phylogenies using maximum parsimony (MP) and maximum likelihood (ML) optimality criteria. Rooted MP, ML, and Bayesian phylogenetic trees were obtained by analyzing the nucleotide sequences of cytochrome oxidase subunit I, 18S rDNA, and 16S rDNA genes, separately and in combination. Representatives of 34 species distributed among seven extant genera were investigated. Our character evolution analyses, combined with recent ontogenetic and ultrastructural evidence, indicate that the organism at the base of the myzostome tree would have had six body segments and five pairs of polychaete-type parapodia, and that two lineages emerged from it: one comprising parasites, with large females and dwarf males, which gave rise to the extant *Pulvinomyzostomum* and *Endomyzostoma* species, and a second lineage comprising simultaneously hermaphroditic ectocommensals, from which all other extant myzostome taxa probably evolved.

Additional key words: character evolution, phylogeny, symbiosis, commensalism

The Myzostomida are one of the most enigmatic of the protostome taxa. With ~170 described species, myzostomes are small, soft-bodied marine worms whose position in the Metazoa has been shifted among groups as diverse as annelids, flatworms, and arthropods since their discovery (for a review, see Eeckhaut & Lanterbecq 2005). Recently, in agreement with morphological characters (Rouse & Fauchald 1997), but in contrast to earlier studies (Eeckhaut et al. 2000), molecular data analyses have begun strongly to support the position that myzostomes are part of the annelid radiation (Bleidorn et al. 2007). Except during their planktonic larval stage, myzostomes are exclusively associated with their host echinoderms and signs of their activities, even if they are not universally accepted as such, are present

on fossil crinoids dating back to the Jurassic (Radwanska & Radwanski 2005), Pennsylvanian (Meyer & Ausich 1983), Silurian (Brett 1978), and also perhaps Ordovician (Warn 1974) periods. Myzostomes have thus evolved intimately with echinoderms, especially crinoids, with which they entered into symbiosis ≤300 million years ago. Currently, most myzostome species (>90%) are ectocommensals on comatulid crinoids, and their anatomy is such that they cannot leave their host to move on the surrounding substrata (Lanterbecq et al. 2007). Parasitism has emerged multiple times from these ectocommensal forms and these parasitic myzostomes infest the integument, gonads, coelom, or digestive system of various echinoderms (Grygier 2000; Lanterbecq et al. 2006). Concomitant with the appearance of these varied symbiotic lifestyles, extant myzostomes show a wide diversity of extravagant body forms (Fig. 1).

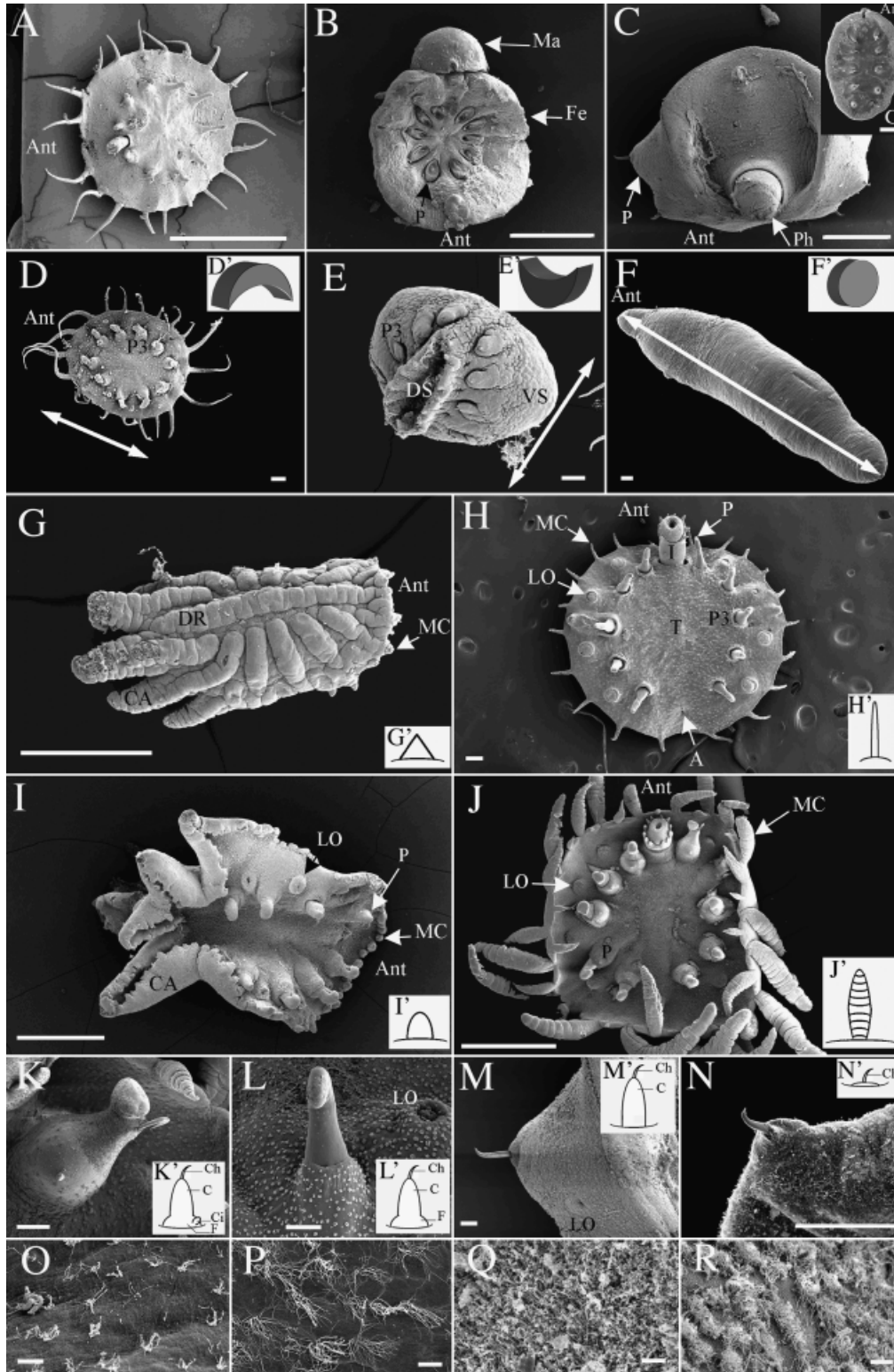
The family-level taxonomy of the Myzostomida (Jägersten 1940) is largely based on the nature of

^a Author for correspondence.

E-mail: deborah.lanterbecq@umh.ac.be

their symbiotic associations. Two orders are distinguished, the Pharyngidea and Proboscidea, the latter represented by a single family, Myzostomatidae, including >90% of the described species, most of them

ectocommensals of crinoids. Pharyngidea includes seven families, of which one is associated with ophiuroids (Protomyzostomidae, including five species, infesting the gonads), two with asteroids (Asteromyzostomidae,



comprising five species, fixed on the body surface of asteroids, and Asteriomyzostomidae, including two species, one parasitic in the digestive system, and the other infesting the coelom), and four with crinoids. These last four families are Pulvinomyzostomidae (represented by a single described species, parasitic in the anterior part of the digestive system), Endomyzostomatidae (~ 10 species infesting the integument), Mesomyzostomatidae (two described species infesting gonads), and Stelechopodidae (one rare species, presumed to be ectocommensal).

To date, two phylogenetic hypotheses exist in the literature to illustrate the relationships within the group: one (Grygier 2000) is based on morphological characters; the other (Lanterbecq et al. 2006) is based on phylogenetic analyses of multiple molecular data sets. The phylogeny of the Myzostomida published by Grygier (2000), which is a revisited analysis of Jägersten's (1940) study, suggested that Pharyngidea contains three to four major clades and is paraphyletic with respect to Proboscidea. The molecular phylogeny of the Myzostomida (Lanterbecq et al. 2006) is based on intensive analyses of multiple DNA data sets (18S rDNA, 16S rDNA, and cytochrome oxidase subunit I [COI]) from 37 crinoid-associated myzostome species (representing nine

genera out of 12). The diversification of symbiotic echinoderm–myzostome associations was investigated by both parsimony- and likelihood-based character reconstruction methods. The phylogenetic analyses indicated that the two orders (Proboscidea and Pharyngidea) do not constitute natural groupings. Character reconstruction analyses suggested that the ancestor of all extant myzostomes was an ectocommensal that first infested crinoids, then asteroids and ophiuroids, and that parasitism in myzostomes emerged multiple times independently.

In the present article, we aim to reconstruct the evolution of morphological features in the Myzostomida in order to (i) assess possible constraints imposed by the various symbiotic ways of life on body form and (ii) estimate the bodyplan of the ancestral myzostome and the organisms that would have comprised the base of the main clades. Our overall intent was not to realize a detailed cladistic analysis using morphological characters, neither to redefine the systematics of Myzostomida at this point, but to examine the evolution of the main characters of the group. Fourteen characters were defined and scored for 44 representatives of 34 myzostome species distributed among seven extant genera, and mapped onto published rooted maximum parsimony (MP) and

Fig. 1. Scanning electron microscopy photographs (and diagrams) illustrating the states of the 14 external morphological characters of adult myzostomes used in the present reconstruction analysis (dv, dorsal view; lv, lateral view; and vv, ventral view). A–C'. Dimorphism versus monomorphism and gonochorism versus simultaneous hermaphroditism. **A.** *Myzostoma nigromaculatum* ECKHAUT et al. 1998 (vv), ectocommensal of crinoids: monomorphic simultaneous hermaphrodite. **B.** *Myzostoma alatum* (vv), ectocommensal of crinoids (dwarf male located on female): monomorphic gonochoric worm. **C, C'.** *Pulvinomyzostomum pulvinar*, endoparasite of crinoid digestive system: dimorphic gonochoric worm; **C,** female (dv); **C',** dwarf male (vv), most of the time located on the ventral side of the female (not shown). **D–H.** Trunk features: arrow indicates trunk length (parallel to the sagittal plane) (in D–F) and P3 indicates parapodia of the third pair (through which a transverse plane was virtually drawn for the inset diagrams). **D.** *Myzostoma ambiguum* (vv), ectocommensal of crinoids; **D',** diagram illustrating the convexo-concave curvature of the trunk. **E.** *Contramyzostoma sphaera* (dv), cysticolous endoparasite living in the crinoid integument; **E',** diagram illustrating the concavo-convex curvature of the trunk. **F.** *Mesomyzostoma* n. sp. 3 (lv), endoparasite living in coelomic cavities close to crinoid gonads; **F',** diagram illustrating the convexo-convex curvature of the trunk. **G–J.** Marginal cirrus features. **G.** *Myzostoma fissum* (dv), ectocommensal sitting mostly on crinoid arms; **G',** diagram illustrating tooth-shaped cirrus. **H.** *Myzostoma cirriferum* LEUCKART 1827 (vv), ectocommensal ambulatory on crinoid arms and calyx, with marginal cirri all equal in length; **H',** diagram illustrating its needle-shaped cirri. **I.** *Myzostoma laingense* (vv), ectocommensal settling on crinoid arms; **I',** diagram illustrating its hump-shaped cirri. **J.** *Myzostoma mortenseni* (vv), ectocommensal settling mostly on crinoid calyx, with cirri not all of equal length and presenting a perfect alternation of long and short); **J',** diagram illustrating its club-shaped cirri. **K–L'.** Parapodial cirrus features: **K, L.** Detailed views of well-developed parapodia with or without a basal parapodial cirrus (*M. mortenseni* and *M. cirriferum*, respectively), and diagrams illustrating their structure (**K', L'**). **L–N'.** Parapodium type: **L, M, N.** Detailed views of parapodia of type 1 (from *M. cirriferum*), type 2 (from *M. mortenseni*), and type 3 (from *Mesomyzostoma* sp.), respectively, and respective diagrams illustrating their structure (**L', M', N'**). **O–R.** Body surface. **O, P.** *Myzostoma cirriferum*: detailed dv and vv, respectively, illustrating the sparse ciliature. **Q, R.** *Notopharyngoides aruensis*, endoparasite located in the anterior part of a crinoid digestive system: detailed dv and vv, respectively, illustrating the dense ciliature. Scale bars: A, B, C, G, I, J = 1 mm; D, E, F, H, K, L, M, N = 100 µm; C' = 120 µm; O, P, Q, R = 10 µm. a, ano-genital pore; ant, anterior part of the body; c, parapodial cone; ca, caudal appendages; ch, parapodial chaeta; dr, dorsal ridge; ds, dorsal side; f, parapodial fold; fe, female; i, introvert; lo, lateral organ; ma, male; mc, marginal cirrus; p, parapodium; p3, parapodium of the third pair; ph, pharynx; t, trunk; vs, ventral side.

maximum likelihood (ML) (Bayesian) phylogenetic trees (Lanterbecq et al. 2006) to realize the character reconstruction analysis.

Methods

Studied species

Most of the myzostomes for this study were collected along with their crinoid hosts via SCUBA dives. They were isolated from living crinoids and (for each species) some specimens were preserved in 100% ethanol (for DNA extraction), in 3% glutaraldehyde in sodium cacodylate buffer, or in Bouin's fluid for histology. Others were fixed in 1% osmium tetroxide in seawater for scanning electron microscopy (SEM). SEM samples were dehydrated in a graded ethanol series, dried using the critical point method (using CO₂ as the transition fluid), mounted on aluminum stubs, coated with gold in a sputter coater, and observed with a JEOL JSM 6100 scanning electron microscope (Jeol Ltd., Tokyo, Japan).

For the present study, 34 species were examined, 26 of which have already been described in the literature while eight are new to science (Appendix 1). Seven genera (out of 12) are included in the study. The genera *Protomyzostomum* and *Asteromyzostomum* (sequenced only for a very short fragment; see Lanterbecq et al. 2006), *Mycomyzostoma* (represented by a single deep-sea species; Eeckhaut 1998), *Asteriomyzostomum* and *Stelechopus* (including a total of only three poorly known species), as well as some morphologically distinct species classified in *Myzostoma* species-groups (Grygier 1990, 1992), for which no molecular data were available, are missing.

Phylogenetic analyses

Myzostome relationships were analyzed using molecular phylogenetic inference methods explained in detail in Lanterbecq et al. (2006). DNA sequences used for estimating myzostome phylogeny were the nuclear small ribosomal subunit (18S rDNA), the mitochondrial large ribosomal subunit (16S rDNA), and mitochondrial COI. MP (in PAUP*4.0b4a, Sinauer Associates, Inc., Sunderland, MA, USA; Swofford 1998), ML (in PAUP*4.0b4a and Metapiga 1.0.2b, http://www.lanevol.org/LANE/bioinformatics_&_software.html; Lemmon & Milinkovitch 2002), and Bayesian analyses (MrBayes v3.0b4, <http://mrbayes.csit.fsu.edu>; Ronquist & Huelsenbeck 2003) were performed on the combined data sets.

Character reconstruction

An increasingly popular method for inferring ancestral states is mapping characters of living organisms onto phylogenetic trees. Although this method has several flaws (see Cunningham et al. 1998; Omland 1999; Ronquist 2004; Crisp & Cook 2005), it is nonetheless a powerful method for assessing features of character transformations. This method is used quite often in evolutionary biology to present the evolution of the morphological (or behavioral) characters of existing species (or fossil organisms when data are available). The aims of this method are (i) to test hypotheses of the way in which characters evolved and (ii) to propose ancestral states, for assessing both the degree of homoplasy in traits and whether a trait contains phylogenetic information or not. This method requires (i) that a reliable phylogenetic analysis has been performed on the group under study and (ii) that character states of various life traits be mapped onto the phylogenetic tree under the rules of an optimality criterion. Some authors favor a "total evidence" approach in combining molecular and morphological data (see Fitzhugh 2006), including those features to be traced (see de Queiroz 1996), which may introduce a bias in the analysis.

In contrast to a similar recent study on Clitellata (Marotta et al. 2008), which included morphological and molecular data in their total evidence approach, we deliberately decided to exclude morphological characters of the phylogenetic inference to (i) ensure the independence of the data sets used to infer the phylogenetic trees from those used in the character reconstruction analyses and (ii) to prevent a possible issue of circularity (or bias) introduced in the analyses. There is also relatively little phylogenetic signal to be gained from the few morphological characters (14 in total) we use here. Even if a total evidence approach would hypothetically help to resolve some nodes of the myzostome tree, we do not consider that in the robustness of this approach if the ultimate goal is to map morphological characters, because circular reasoning and tautology would result.

Morphological characters and states for myzostomes (Appendix 1) were mapped onto trees derived from MP and Bayesian analyses using MP and ML as the optimality criteria. The most parsimonious explanation for the histories of morphological characters was inferred and visualized using MacClade 4.0 (Sinauer Associates; Maddison & Maddison 2000) under default settings. Because branch lengths are required in ML mapping analyses, the ML optimality criterion was used only in analyses on the Bayesian tree, and the results were then compared with the re-

sults obtained in MP mapping analyses of both trees. Mesquite 1.0 (<http://mesquiteproject.org>; Maddison & Maddison 2004) was used to reconstruct the evolution of characters under ML criteria, using the Markov k-state 1-parameter model, which corresponds to Lewis's (2001) Mk model.

Because of the obscure relationships of myzostomes with other metazoans, outgroup taxa were not considered in the present character evolution analysis, the ultimate goal of the study being the analysis of the evolution of the main characters within the group. However, we emphasize that the phylogenetic trees used in the character evolution analysis are rooted trees, as several outgroup taxa were tested and used to root the ingroup tree (see Lanterbecq et al. 2006 for details).

Fourteen characters were used in our analyses (see Appendix 1). All were based on adult attributes as follows: (1) dimorphism versus monomorphism, (2) gonochorism versus simultaneous hermaphroditism, (3) trunk shape, (4) trunk curvature, (5) number of marginal cirri, (6) shape of marginal cirri, (7) relative length of marginal cirri, (8) number of lateral organs, (9) type of parapodia, (10) parapodial cirri, (11) body ciliation, (12) introvert, (13) dorsal ridges, and (14) caudal appendages. These are major characters that are most evident when observing myzostomes alive and/or with SEM on preserved specimens. They are also the most pertinent to assess the possible constraints imposed by the various symbiotic ways of life on body form, and to estimate the bodyplan of the organisms that would have comprised the base of the main clades. Other characters (e.g., number of buccal cirri, details of positioning of lateral organs, presence of villose U-shaped pads on the parapodia, etc.) could be considered in other studies having aims other than those of the present work.

All these characters were scored based on observations of photographs of live organisms and direct observations of living and/or fixed organisms using light and scanning electron microscopes. The only exception was the male stage in *Endomyzostoma tenuispinum* GRAFF 1884, for which no individuals were sampled and the scoring of character states was based on the literature alone. Gonochoric species (Fig. 2) were split into two operational taxonomic units (OTUs) or taxa, one going to the male stage and the other to the female stage (Figs. 4–9), to allow full character mapping. This did not apply, of course, to the first two characters (i.e., dimorphism vs. monomorphism, and gonochorism vs. simultaneous hermaphroditism; Fig. 2, respectively). Characters were coded either as binary or multistate (see Appendix 1).

Morphological analysis

Morphism and sexes. Most myzostomes are simultaneous hermaphrodites (Fig. 1A), but in a few, the sexes are separated. These species are probably gonochoric, but protandric hermaphroditism, with male individuals being found with females on the same hosts, is also a state that could occur in these myzostomes (Fig. 1B,C). In our sample of taxa, 29 specimens (belonging to 25 species) were simultaneous hermaphrodites, and the status of three specimens (belonging to three species) was unavailable and coded as missing. Among the gonochoric forms, dimorphism in size and shape exists between males (called dwarf males) and females in four of the six species. The two other gonochoric species, *Myzostoma glabrum* LEUCKART 1842 and *Myzostoma alatum* GRAFF 1884 (Fig. 1B), are monomorphic, although the males are reduced in size and attached to the antero-dorsal part of the female (Eeckhaut & Jangoux 1992).

1. Dimorphism versus monomorphism: (0) dimorphic; (1) monomorphic; (?) missing or unavailable data.
2. Gonochorism versus simultaneous hermaphroditism: (0) gonochoric; (1) simultaneous hermaphrodites; (?) missing or unavailable data.

Because ML reconstruction requires that all character states be non-ambiguous (Maddison & Maddison 2004), the three undescribed species that had unknown character states (*Endomyzostoma* n. sp. 1, *Endomyzostoma* n. sp. 2, and *Endomyzostoma* n. sp. 3) were removed from the ML analysis.

Trunk features. The body of most myzostomes consists of a trunk (see Fig. 1H) and an anterior cylindrical introvert (also called a proboscis), the latter being absent in some species (e.g., *Pulvinomyzostomum pulvinar* GRAFF 1884 has no introvert but exhibits an extrusible pharynx, Fig. 1C). The myzostome trunk has a wide diversity of shapes, and was characterized here on the basis of two parameters: shape and curvature. The trunk shape of a myzostome can be characterized via a ratio between its length (L) and its width (W). The length of the trunk was measured as the distance between the anterior and the posterior margins in the sagittal plane (Fig. 1D–F). The width was measured as the transverse distance between the margins at the level of the third pair of parapodia (corresponding for most myzostomes to the middle of the body). If the myzostome was not flat, or if it was rolled up, the distances (length and width) were measured, compared with

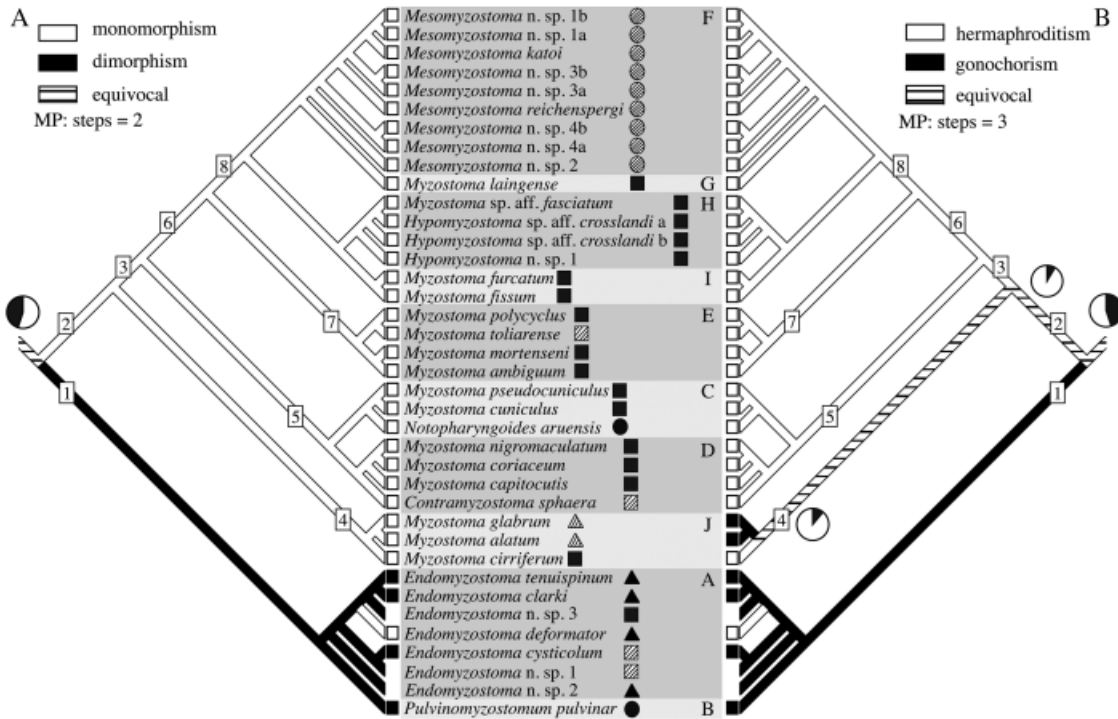


Fig. 2. Maximum parsimony (MP) character reconstruction (on the MP tree) of “dimorphism versus monomorphism” (A), and “gonochorism versus simultaneous hermaphroditism” (B). The MP tree (bootstrap 50% majority rule consensus tree) was obtained with a data set including three genes (18S rDNA, 16S rDNA, and cytochrome oxidase subunit I) (Lanterbecq et al. 2006). Squared numbers refer to main clades and letters (A–J) emphasize groups that were observed in most of the analyses. Bootstrap values (left) and Bayesian posterior support (right) were obtained for the main clades as follows: 1 (73/1.00), 2 (100/1.0), 3 (48/0.56), 4 (61/0.61), 5 (10/–), 6 (11/–), 7 (37/0.84), 8 (61/0.56), A (100/1.00), D (47/1.00), C (55/0.62), F (80/1.00), I (77/1.00), and H (16/–). Absence of a square in front of the three undescribed species, *Endomyzostoma* n. sp. 1, *Endomyzostoma* n. sp. 2, and *Endomyzostoma* n. sp. 3, indicates coding “?” in the MP analysis (these species were deleted in the maximum likelihood [ML] analysis). For the equivocal branches of the MP tree, a pie diagram shows the ML probability for the states mapped onto the Bayesian tree. The six lifestyles are illustrated by symbols to the right of the name species: hatched square, cysticolous parasite; hatched circle, gonad endoparasite; hatched triangle, ectoparasite; black square, ectocommensal; black circle, digestive system parasite; black triangle, gallicolous parasite.

literature descriptions, and the mean values were taken into account to score the characters. Based on the measurements, three discrete states were recognized: almost as long as wide ($0.66W < L < 1.5W$) (Fig. 1D), wider than long ($W \geq 1.5L$) (Fig. 1E), or longer than wide ($L \geq 1.5W$) (Fig. 1F). Trunk curvature was estimated from a transverse section through the trunk at the level of the third pair of parapodia (Fig. 1D–F). Dorsal and ventral orientation was taken into account to describe the section, which might be convexo-concave (i.e., dorsal is convex and ventral is concave, Fig. 1D’), concavo-convex (i.e., dorsal is concave and ventral is convex, and the myzostome is folded up, Fig. 1E’), or convexo-convex (i.e., dorsal and ventral are both convex and the animal is circular in cross-section, Fig. 1F’).

3. Trunk shape: (0) $L \approx W$; (1) $W > L$; (2) $L > W$.

4. Trunk curvature: (0) convexo-concave; (1) concavo-convex; (2) convexo-convex.

Cirrus features. Many myzostomes have cirri around their trunk margin (Fig. 1). Typically, there are 20 (= ten pairs, Fig. 1A,D,H), but sometimes more (Fig. 1I,J) (> 100 in some species, not illustrated), and with less in others (not shown). Some species do not have cirri at all (Fig. 1C). Myzostome marginal cirri were characterized here on the basis of three parameters: their number, their shape, and their relative length. Tooth-shaped cirri are triangular trunk projections (Fig. 1G’). Hump-shaped cirri are hemispherical trunk projections (Fig. 1I’). Needle-shaped cirri are $\geq 10\times$ longer than their basal diameter, and they taper gradually from the base to the end (Fig. 1H’). The word “needle” is used to illustrate the general shape of the cirri, and does not absolutely refer to their

stiffness (they are in fact very flexible). Club-shaped cirri are stout, much longer than wide but thicker in the middle than at either end (Fig. 1J'). When cirri are present around the trunk margin, they may be equal (Fig. 1H) or unequal in length. For the latter condition, we observed whether there was an alternation of two markedly different lengths (Fig. 1J), or whether the anterior/posterior pairs were $\geq 1.5 \times$ longer than the lateral ones (Fig. 1D).

5. Number of marginal cirri: (0) >20 (ten pairs); (1) $=20$; (2) absent; (3) <20 .
6. Shape of marginal cirri: (0) tooth; (1) hump; (2) needle; (3) club; (4) absent.
7. Length of marginal cirri: (0) equal; (1) not equal; (2) absent.

Four shapes of cirri are thus considered here based on their external similarity, whereas there is no evidence that the rounded humps of a scalloped body margin are homologous to the usual marginal cirri. There are actually some debates as to the homology of these structures, and no detailed histological, ultrastructural, or developmental analyses have been performed yet to prove their homology in structure or function.

Besides the marginal cirri, hump-shaped or pointed parapodial cirri have been described in some myzostome species (Fig. 1K, K'). These will be discussed in "Parapodia."

Lateral organs. Most myzostomes have dome-shaped (Fig. 1L) or slit-like (Fig. 1M) sensory lateral organs. They are usually present in four pairs, often alternating with parapodia (Fig. 1H–J). In a few cases, they are absent (Fig. 1F) or there are >4 pairs (in *P. pulvinar*, illustrated in Fig. 1C).

8. Number of lateral organs: (0) absent; (1) 4 pairs; (2) >4 pairs.

Parapodia. Myzostomes have five pairs of unarticulated appendages, usually called parapodia, located along some part of the length of the trunk. Each parapodium is conical, with a hook-shaped chaeta protruding distally (Fig. 1K'–N'). The parapodia are generally located ventrally (Fig. 1D, H–J), but sometimes in a lateral position (Fig. 1C), or close to the dorsal side (Fig. 1E). Three types of parapodia (character 9) can be differentiated in the myzostomes we studied. They may be well developed, characterized by the presence of a basal parapodial fold (Fig. 1K, L). The parapodial cone is stout, with a strong, curved chaeta protruding apically (Fig. 1L'). Parapodia of the second type (Fig. 1M) are less developed, and lack the

parapodial fold (Fig. 1M'). Parapodia of the third type (Fig. 1N) are very poorly developed, and often only represented by the hooked chaeta extending from a button-like protrusion (Fig. 1N'). Parapodial cirri (character 10), characterizing some parapodia of type 1, may be present (Fig. 1K, K') or absent (Fig. 1L, L'). If present, the cirrus is located medially on the basal fold of the parapodium.

9. Parapodia: (0) type 1; (1) type 2; (2) type 3.
10. Parapodial cirrus: (0) absent; (1) present.

Body ciliature. Non-ciliated and ciliated cells form most of the myzostome epidermis. Ciliated cells have a shape and size similar to covering cells and bear 20–50 cilia (10–20 μm long). Cilia are generally grouped in patches on the body surface of myzostomes (Fig. 1O, P; illustrating the dorsal and ventral ciliature, respectively), but the body is sometimes covered uniformly with cilia (Fig. 1Q, R). Ciliated cells are sparse (with a ratio of ciliated cells to non-ciliated cells of $\sim 1:5$) or the trunk is almost totally covered by cilia (with a ratio of 1:1).

11. Body surface (ciliature): (0) sparse; (1) dense.

Introvert. An introvert, or proboscis, representing the entire anterior end of the larva, is present in all representatives of the order Proboscidea (Fig. 1H, J). This has been inferred to be absent in Pharyngidea (Jägersten 1940; Grygier 2000) (Fig. 1C, E, F), which instead have a protrusible pharynx (e.g., *P. pulvinar*, Fig. 1C). *Contramyzostoma* has previously been considered, with some hesitancy, to be part of the Pharyngidea (see Grygier 2000); however, *Contramyzostoma sphaera* ECKHAUT et al. 1998 has an introvert. Also, the type-species of the genus, *Contramyzostoma bialatum* ECKHAUT & JANGOUX 1995, has an arrangement of the salivary gland cells close to what can be observed in *Myzostoma* (Eckhaut & Jangoux 1995).

12. Introvert: (0) absent; (1) present.

Particular appendages. Sagittal, radial, and/or transverse dorsal ridges are present in some of the myzostomes studied here (Fig. 1G); other kinds of dorsal ornamentation are found in other species. Caudal appendages, or lobes, sometimes bearing cirri, and into which the internal organs penetrate (Grygier 2000), are also present in some species (Fig. 1G, I). The shape and number of caudal appendages vary; there may be a single upturned or furled lobe or several triangular or finger-like lobes (unlikely to be homologous).

13. Dorsal ridges: (0) absent; (1) present.
 14. Caudal appendages: (0) absent; (1) present.

Results

Myzostome phylogeny

Figure 2A shows an MP bootstrap 50% majority rule consensus tree arising from analysis of the three-gene data set (Lanterbecq et al. 2006: fig. 4). The analyses using outgroup taxa, tested together or separately (five Annelida, two Plathelminthes, two Rotifera, and two Acanthocephala), supported the rooting of the myzostome clade (Lanterbecq et al. 2006: fig. 3) on a lineage including all the *Endomyzostoma* species, endoparasitic species living in galls, plus *Pulvinomyzostomum pulvinar*, an endoparasitic species living in the mouth and the digestive tube (clade 1, Fig. 2A). The Myzostomida can be divided into main two clades: one (clade 1) comprising all *Endomyzostoma* species (clade A) with *P. pulvinar* (clade B) as a sister group and the second clade (clade 2) comprising all other myzostome species. Clade 2 can be split into two clades (3 and 4). Clade 4 con-

tains three European species that were found on the body surface of comatulid crinoids. The other myzostomes (clade 3) are all Indo-West Pacific species divided into two groups: one of seven species (clade 5) and the other of 20 species (clade 6). Clade 5 contains five species of *Myzostoma*, all ectocommensals, *Notopharyngoides aruensis* REMSCHEID 1918, a crinoid mouth (and digestive system) parasite, and *Contramyzostoma sphaera*, a parasite of crinoid integument. Clade 6 contains two main clades: one comprised of four *Myzostoma* ectocommensals (clade 7) and the other (clade 8) of species from three different genera (*Myzostoma*, *Mesomyzostoma*, and *Hypomyzostoma*). *Mesomyzostoma*, crinoid intra-gonadal parasites, and the ectocommensal *Hypomyzostoma* species are both monophyletic genera with different *Myzostoma* species as their respective sister groups. The sister group to the *Mesomyzostoma* clade is *Myzostoma laingense* EECKHAUT et al. 1998, a large species generally found on crinoid arms. *Hypomyzostoma* clusters with *Myzostoma fissum* GRAFF 1884 and *Myzostoma furcatum* GRAFF 1887, two species with caudal appendages that resemble crinoid pinules.

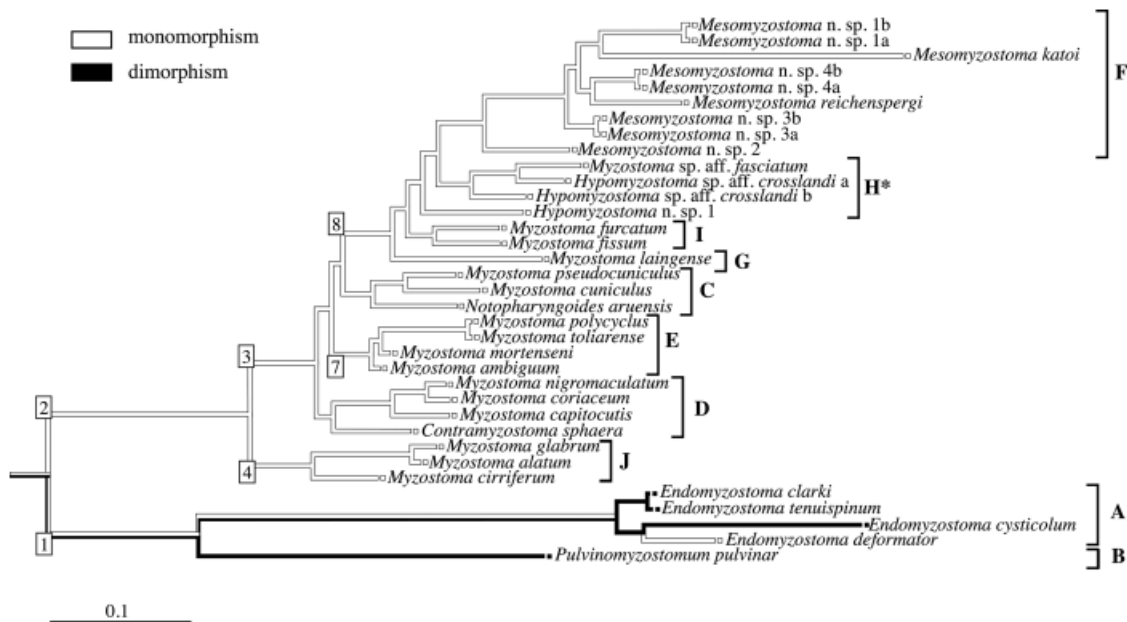


Fig. 3. Maximum likelihood (ML) character reconstruction (on the Bayesian majority rule consensus tree) of “dimorphism versus monomorphism.” The Bayesian tree was obtained with a data set including three genes (18S rDNA, 16S rDNA, and cytochrome oxidase subunit I) (Lanterbecq et al. 2006). Square-framed numbers refer to main clades, and letters (A–J) denote groups that were observed in most of the analyses. Bootstrap values (left) and Bayesian posterior support (right) were obtained for the main clades as follows: 1 (73/1.00), 2 (100/1.0), 3 (48/0.56), 4 (61/0.61), 5 (10/–), 6 (11/–), 7 (37/0.84), 8 (61/0.56), A (100/1.00), D (47/1.00), C (55/0.62), F (80/1.00), I (77/1.00), and H (16/–). H* indicates the paraphyletic status of *Hypomyzostoma*. Branch lengths are proportional substitutions per site (see scale in figure). The three undescribed species, *Endomyzostoma* n. sp. 1, *Endomyzostoma* n. sp. 2, and *Endomyzostoma* n. sp. 3, coded “?” in the maximal parsimony analysis, were deleted in the ML analysis.

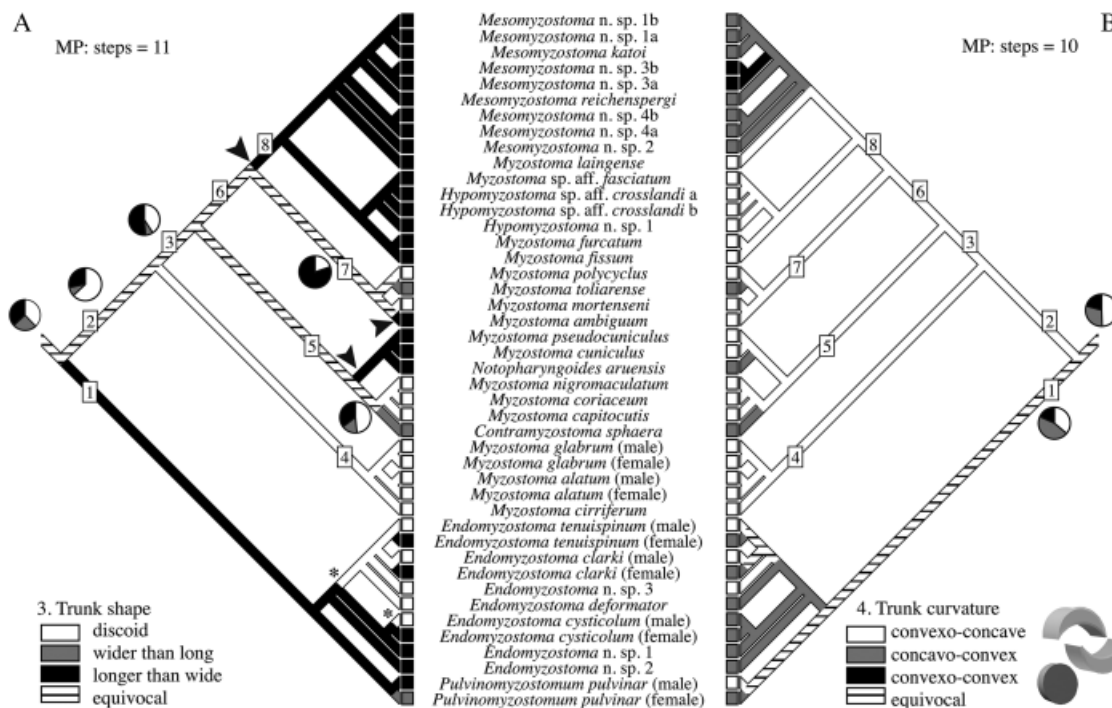


Fig. 4. Maximum parsimony (MP) character reconstruction (on the MP tree) of the evolution of the trunk shape (A) and the trunk curvature (B). Square-framed numbers refer to the main clades observed in most of the molecular analyses (Lanterbecq et al. 2006). For the equivocal branches of the MP tree, a pie diagram shows the maximum likelihood (ML) probability for the states mapped onto the Bayesian tree. The number of steps required to explain the MP evolutionary pattern is mentioned. The three arrows show that the trunk may have changed from discoidal to longer than wide 3×. The asterisks show the transformation from the elongate to discoidal state.

The relationships among myzostomes in the Bayesian tree (Fig. 3) are somewhat similar to those observed on the MP tree: a basal split into clades 1 and 2, and the major lineages identified within them (clades A–J) are also present, except that *Hypomyzostoma* appears to be paraphyletic (Fig. 3: H*). Clades 5 and 6 from the MP analysis were not recovered. Other differences appear in the positions of *M. laingense*, *Endomyzostoma deformatum* GRAFF 1884, and *Myzostoma ambiguum* GRAFF 1887 (Lanterbecq et al. 2006: fig. 5).

Character-mapping analyses

The MP and ML reconstructions show similar overall inferences, and so only the MP reconstructions on the MP tree (Fig. 2A) are shown in the figures. These results are also compared with the results obtained with the same reconstructions (MP) on the Bayesian tree (Fig. 3), and the number of steps required to explain the MP evolutionary pattern is mentioned in the figures. The results of the analysis using ML as an optimality criterion realized on the Bayesian tree are illustrated as “pies” on “equivocal”

transformation areas of the MP tree (Figs. 4–9), when it is possible to do so. (Some nodes are present in the MP tree that do not exist in Bayesian tree, e.g., nodes 5 and 6; see also the Bootstrap and Bayesian posterior values of the main clades in the legend of Fig. 2.)

Monomorphism versus dimorphism. Monomorphism (white in Figs. 2A, 3) characterizes all species of clade 2 (extant species and the most recent common ancestral state for the clade) and dimorphism (black in Figs. 2A, 3) appears at the base of clade 1, followed by a reversal to monomorphism in *E. deformatum*. The state for the ancestral myzostome (the root of the tree) is equivocal in MP analyses, but the ML analysis shows monomorphism as more likely (55%) (Figs. 2A, 3).

Gonochorism versus hermaphroditism. Gonochorism (in black in Fig. 2B) is the unequivocal condition for clade 1, with a switch to simultaneous hermaphroditism (in white in Fig. 2B) with the appearance of *E. deformatum*. Simultaneous hermaphroditism characterizes most organisms of clade 2, except for gonochorism in *Myzostoma glabrum* and *Myzostoma alatum*. The ancestral myzostome

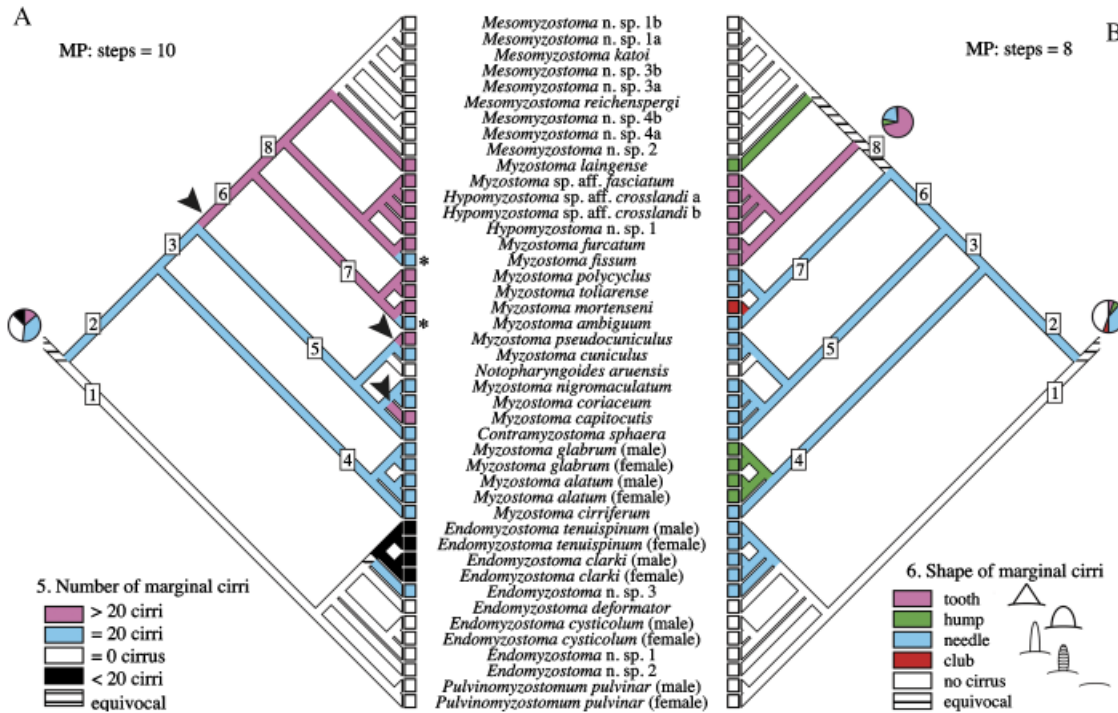


Fig. 5. Maximum parsimony (MP) character reconstruction (on the MP tree) of the evolution of the number of marginal cirri (A) and the shape of marginal cirri (B). Square-framed numbers refer to the main clades observed in most of the molecular analyses (Lanterbecq et al. 2006). For the equivocal branches of the MP tree, a pie diagram shows the maximum likelihood (ML) probability for the states mapped onto the Bayesian tree. The three arrows show that the number of marginal cirri may have increased 3 \times , with two subsequent reversals to 20 cirri shown by asterisks; however, this is only one of several possible most parsimonious transformations.

condition and the one for the bases of clades 2 and J are equivocal under parsimony, but simultaneous hermaphroditism is the most likely for all three (55%, 91%, and 88%, respectively).

Trunk shape. A trunk that is wider than long (tracing in light gray, Fig. 4A) appears 3 \times independently (in the female stage of *P. pulvinar*, in *C. sphaera*, and in *Myzostoma toliarense* LANTERBECQ & EECKHAUT 2003). The trunk condition at the base of clade 1 (female and male stages) is the elongate state (longer than wide, black in Fig. 4A). Within this clade, the trunk changes to discoidal (in white) twice (marked by asterisks), with a reversal to a trunk longer than wide in the females of *Endomyzostoma tenuispinum* and *Endomyzostoma clarki* MCCLENDON 1906. The trunk of the myzostome at the base of clade 2 may be discoidal (ambiguous in MP, but most likely with 63%) and is longer than wide in three taxa (highlighted by arrows), allowing for various equally parsimonious transformations. The trunk shape of the ancestral myzostome could not be resolved in this study (equivocal in MP; discoidal or elongate trunk evenly likely, 38% and 37%, respectively).

Trunk curvature. A thread-like trunk with a convexo-convex (circular) section (illustrated in black, Fig. 4B) appears once, in *Mesomyzostoma* n. sp. 3. A trunk with a concavo-convex section (mapped in gray, Fig. 4B) unequivocally appears 4 \times in clade 2 (in *C. sphaera*, *N. aruensis*, *M. toliarense*, and *Mesomyzostoma*) and also characterizes all females of clade 1, the male stage of *Endomyzostoma cysticolum* GRAFF 1883, the hermaphrodite *E. deformatum*, and *Endomyzostoma* n. sp. 1 and 2 (the sexual condition is unknown for these two last species). The males of clade 1 (except *E. cysticolum*) exhibit a convexo-concave trunk, as does *Endomyzostoma* n. sp. 3. The ancestral state of the myzostome ancestor and at the base of clade 1 is equivocal.

Number of marginal cirri. The plesiomorphic condition for clade 1 is the absence of marginal cirri (white, Fig. 5A). Within clade 1, there are several equally parsimonious transformations to either the 20-cirri state (in blue) for *Endomyzostoma* n. sp. 3 or <20 cirri (in black) for the clade containing *E. clarki* and *E. tenuispinum*. Clade 2 shows the 20-cirri state as the ancestral state (Fig. 5A), with the number of marginal cirri increasing 3 \times independently (marked

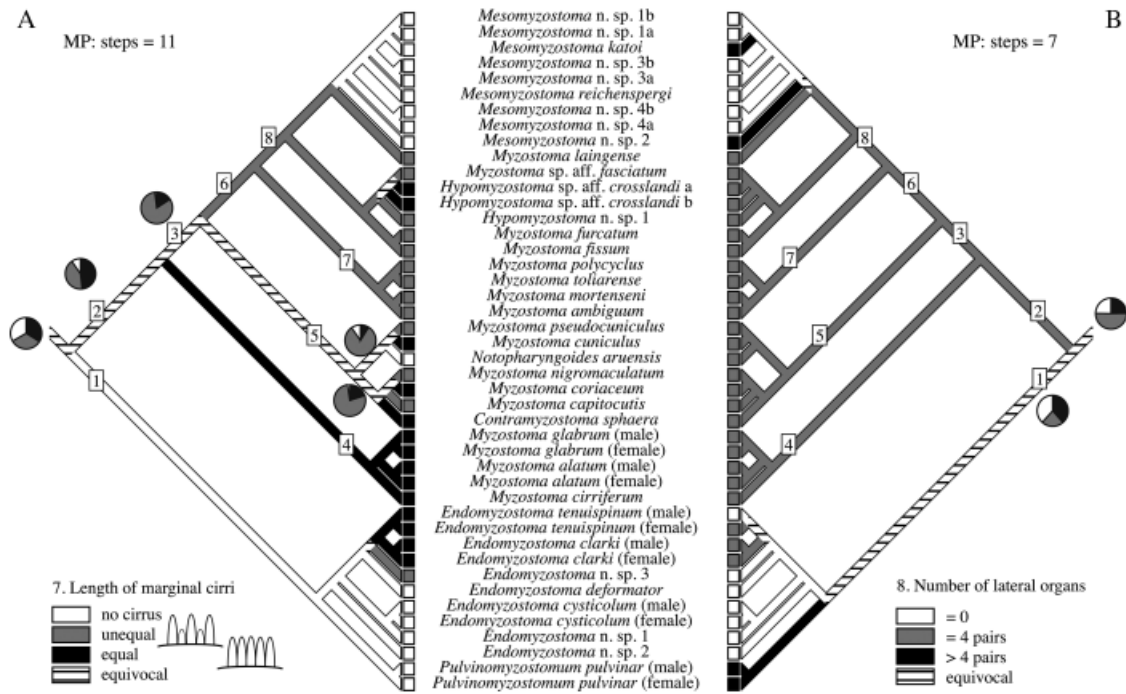


Fig. 6. Maximum parsimony (MP) character reconstruction (on the MP tree) of the evolution of the length of the marginal cirri (A) and the number of lateral organs (B). Square-framed numbers refer to the main clades observed in most of the molecular analyses (Lanterbecq et al. 2006). For the equivocal branches of the MP tree, a pie diagram shows the maximum likelihood probability for the states mapped onto the Bayesian tree.

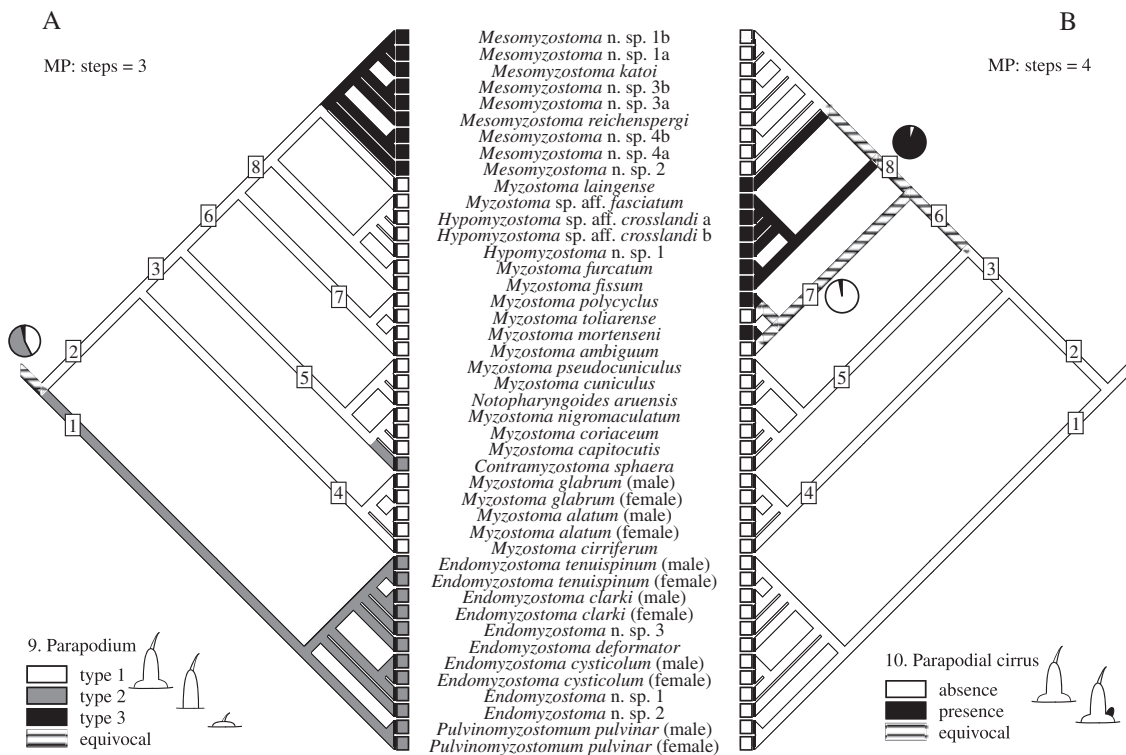


Fig. 7. Maximum parsimony (MP) character reconstruction (on the MP tree) of evolution the type of parapodia (A) and the presence/absence of parapodial cirri (B). Square-framed numbers refer to the main clades observed in most of the molecular analyses (Lanterbecq et al. 2006). For the equivocal branches of the MP tree, a pie diagram shows the maximum likelihood probability for the states mapped onto the Bayesian tree.

by arrows), with two subsequent reversals to 20 cirri (in *M. fissum* and *M. ambiguum*, highlighted by asterisks). Marginal cirri are lost in *Mesomyzostoma* species and in *N. aruensis* (in white). The state of the ancestral myzostome is equivocal, even in ML analyses. The most likely scenarios are an ancestor exhibiting either 20 cirri or none (38% and 35%, respectively).

Shape of marginal cirri. The absence of cirri is the ancestral state for clade 1, with needle-shaped cirri as ancestral for clade 2 (Fig. 5B). There are several possible transformations for clade 8. If present in the ancestral myzostome, marginal cirri were most probably needle shaped (38% in ML analysis).

Length of marginal cirri. The course of variation of cirrus length (when present) is equivocal in much of the tree, with many equally parsimonious transformations (Fig. 6A). The ancestral myzostome condition also cannot be resolved. The ancestral condition for clade 2 may be to have had equal cirri (48% vs. 42% for unequal in ML) that evolved to unequal cirri in clade 3 (83% in ML).

Lateral organs. Most myzostomes have four pairs of lateral organs (gray) and this is the ancestral condition for clade 2 (Fig. 6B). Lateral organs appear to have disappeared twice independently: once in *Mesomyzostoma* (although with an increase in number in *Mesomyzostoma* n. sp. 2, and reappearance of >4 pairs in *Mesomyzostoma katoi* OKADA 1933) and also in most *Endomyzostoma*. The equivocal status of the clade 1 ancestor is not resolved with the ML analysis (none or >4 pairs, 39% and 38%, respectively); however, the myzostome ancestral condition may have been four pairs of lateral organs (51%).

Parapodia. The type of parapodia is equivocal at the base of the tree, but the presence of parapodia of type 2 is most likely (54%) (Fig. 7A). Poorly developed parapodia (type 3) appeared once in *Mesomyzostoma*, medium-sized parapodia (type 2) appeared once at the base of clade 1, and well-developed parapodia (type 1) appeared once at the base of clade 2, with regression into type 2 in *C. sphaera*.

Parapodial cirri. The ancestral myzostome appears to have lacked parapodial cirri (Fig. 7B). There are various most-parsimonious scenarios for the evolution of this feature thereafter. For instance, either they appeared independently several times in clade 2 (in *Myzostoma mortenseni* JÄGERSTEN 1940, *Myzostoma polycyclus* ATKINS 1927, *M. laingense*, and in *Mesomyzostoma*) or they may have appeared once at the base of clade 8, followed by their loss in *Mesomyzostoma* species within clade 8.

Body ciliature. The mapping is fully resolved: the body ciliature becomes uniform and dense 3× with

the appearance of parasitism in the digestive tract (*N. aruensis* and *P. pulvinar*) and gonads (*Mesomyzostoma*) (Fig. 8A).

Introvert. Absence and presence of an introvert in the myzostome ancestor are equally parsimonious possibilities (Fig. 8B). The introvert is unequivocally the condition for clade 2 and is then lost in *Mesomyzostoma*.

Dorsal ridges. They appear either 3× in the MP reconstruction or they may have appeared only once (at the base of clade 8), followed by a reversal in *Mesomyzostoma* and in *Hypomyzostoma* sp. aff. *crosslandi* a and b BOULENGER 1913 (Fig. 9A).

Caudal appendages. Caudal appendages appear 3× independently: in (i) *Myzostoma cuniculus* EECKHAUT et al. 1998 + *Myzostoma pseudocuniculus* LANTERBECQ & EECKHAUT 2003, (ii) in *Myzostoma fissum* + *Myzostoma furcatum*, and (iii) in *M. laingense* (Fig. 9B).

Evolution of the ancestral myzostome bodyplan

Based on the transformations outlined above, we can provide a summary of what the ancestral myzostome condition may have been. This appears to have been a monomorphic simultaneous hermaphrodite (equivocal but most likely) with a discoidal or an elongate convexo-concave trunk. If the trunk margin possessed cirri, they would have been needle shaped and of equal length. Four pairs of lateral organs and presumably five pairs of acirrate parapodia (type 2 parapodia) alternated in position on the ventral side of the trunk. If ciliature was present, it was sparse. It is most likely that no introvert was present, nor any external ornamentation such as dorsal ridges or caudal appendages. Myzostomes then evolved in two distinct lineages: clade 1 (grouping *Pulvinomyzostomum* and *Endomyzostoma* species) and clade 2 (including the remaining myzostomes). The ancestral condition for clade 1 appears to have been a dimorphic gonochoric myzostome, with an elongate concavo-convex trunk lacking marginal cirri. The number of lateral organs is not resolved and the plesiomorphic conditions of acirrate parapodia (type 2), sparse ciliature (if present at all), and lack of introvert, dorsal ridges, and caudal appendages were retained. The ancestral condition for clade 2 can be inferred to have been monomorphic, simultaneously hermaphroditic, and most likely with a discoidal, convexo-concave trunk. The margin had 20 needle-shaped cirri of equal length. Four pairs of lateral organs and five pairs of acirrate parapodia of type 1 (i.e., possessing a basal fold) probably alternated on the ventral side. The ciliature was sparse

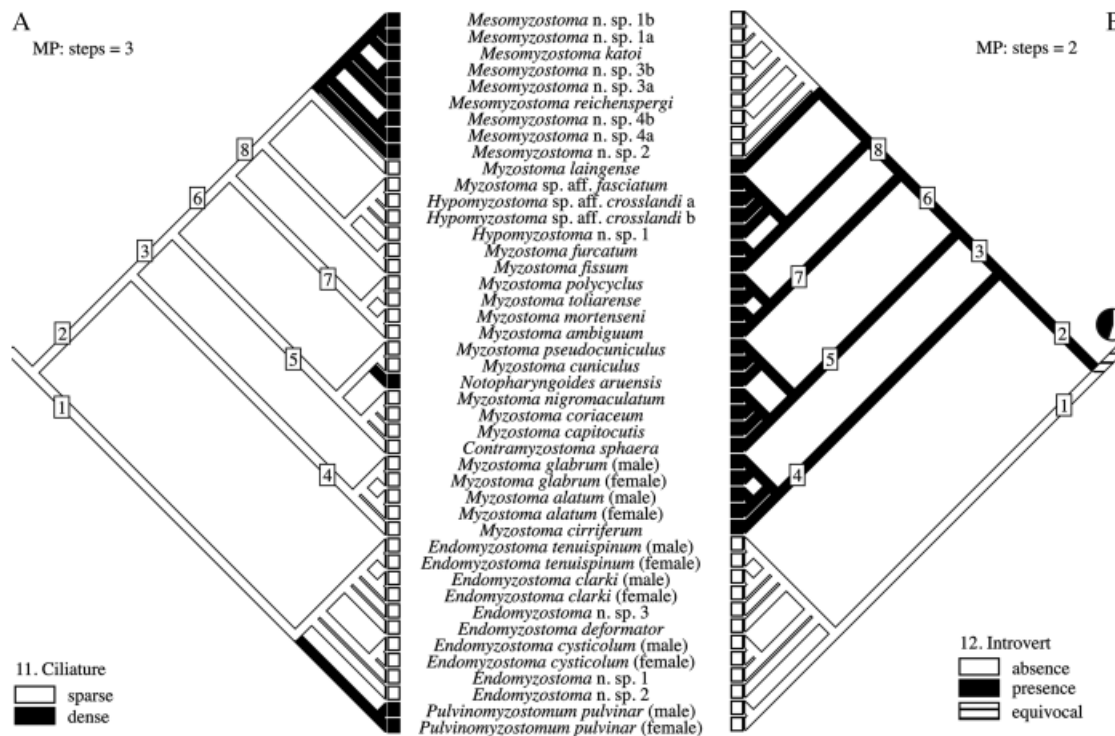


Fig. 8. Maximum parsimony (MP) character reconstruction (on the MP tree) of the evolution of body ciliature (A) and the introvert (B). Square-framed numbers refer to the main clades observed in most of the molecular analyses (Lanterbecq et al. 2006). For the equivocal branches of the MP tree, a pie diagram shows the maximum likelihood probability for the states mapped onto the Bayesian tree.

and the trunk was lacking in both dorsal ridges and caudal appendages. The ancestral condition for clade 2 was to have an introvert.

Discussion

Jägersten (1940) considered myzostomes as a class closely related to Annelida, comprised of two orders, Proboscidea and Pharyngidea, with one and seven families each, respectively (Grygier 2000). One point that is strongly supported in the phylogenetic analyses is that Proboscidea and Pharyngidea are not monophyletic and that the systematics of the Myzostomida need substantial revision (Lanterbecq et al. 2006). Our results suggest that the Myzostomida comprise two main clades: one mainly composed of dimorphic gonochoric species (clade 1, Fig. 2A) and the other exclusively composed of monomorphic simultaneous hermaphroditic species (clade 2, Fig. 2A). We refrain from naming these new clades at present until a more complete sampling of myzostome diversity is achieved. Morphologically distinct species or species groups (Grygier 1990, 1992) currently assigned to *Myzostoma* are not treated in this study. For example, these include round species

with dorsal ridges and ten pairs of minute cirri, like *Myzostoma insigne* ATKINS 1927; irregularly tapering species, like *Myzostoma attenuatum* GRYGIER 1989; and the *Myzostoma intermedium* GRAFF 1884 group, with a cirrus on each of multiple caudal processes.

The dimorphic clade of the present analysis (clade 1) includes two of the seven families that were established in the Pharyngidea: Endomyzostomatidae and Pulvinomyzostomidae. Endomyzostomatidae includes two genera, *Endomyzostoma* and *Mycomyzostoma*, the latter not being represented in our analyses but containing a single dimorphic species that creates galls on deep-sea stalked crinoids (Eeckhaut 1998). The monomorphic clade (clade 2) includes only one family, the Myzostomatidae, in the present analysis. However, we suggest that the remaining pharyngidean families (Protomyzostomidae, Stelechopodidae, Asteriomyzostomidae, and Asteromyzostomidae) should be placed in clade 2 based on the monomorphic status of their species, even though we did not have access to material for all of them. The two described species of Asteriomyzostomidae, *Asteriomyzostomum asteriae* MARENZELLER 1895 and *Asteriomyzostomum fisheri* WHEELER 1905 are functional hermaphrodites at the adult stage, as is

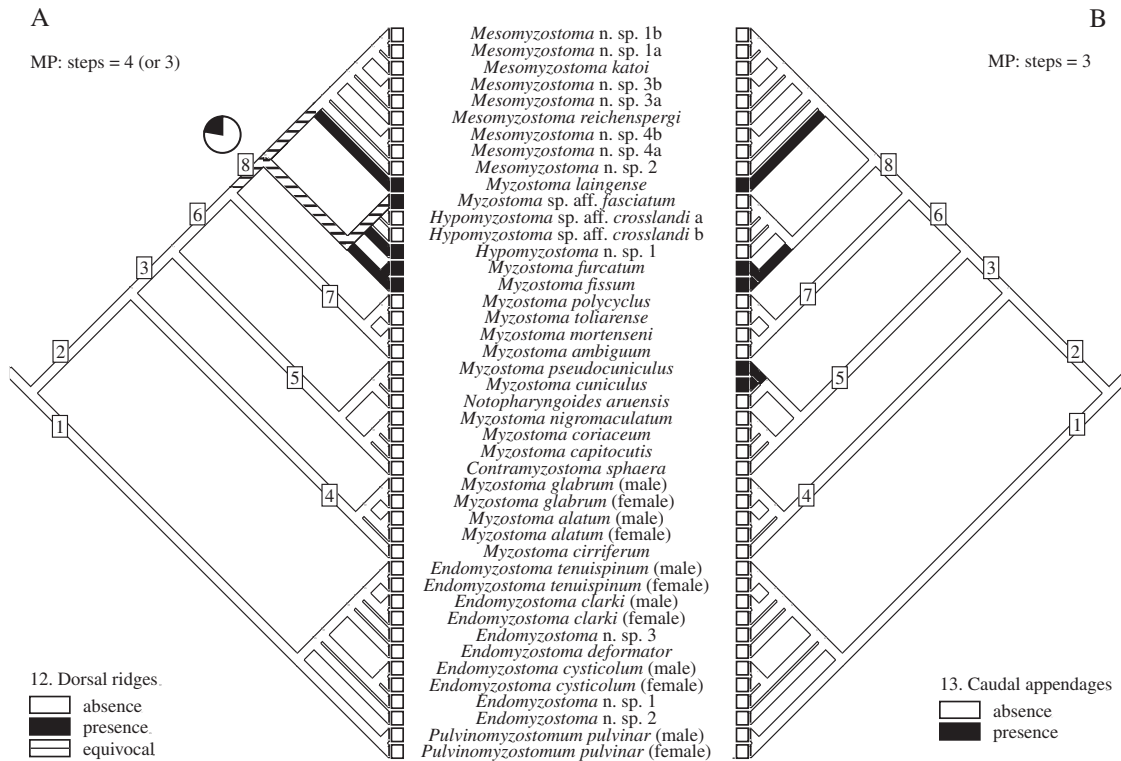


Fig. 9. Maximum parsimony (MP) character reconstruction (on the MP tree) of dorsal ridges (A) and caudal appendages (B). Square-framed numbers refer to the main clades observed in most of the molecular analyses (Lanterbecq et al. 2006). For the equivocal branches of the MP tree, a pie diagram shows the maximum likelihood probability for the states mapped onto the Bayesian tree.

the single species of Stelechopodidae, *Stelechopus hyocriini* GRAFF 1884 (Grygier 2000). Protomyzostomidae, two members of which were found in clade 2 in the molecular study (Lanterbecq et al. 2006), are endoparasites living in the gonads, coelomic cavities, or cysts on the arms of ophiuroids. Members of the last family, the Asteromyzostomidae, are asteroid ectoparasites, and one representative, *Asteromyzostomum* sp., was found in clade 7 in the molecular study (Lanterbecq et al. 2006). Proboscidea (comprised of only the Myzostomatidae in Jägersten 1940) forms a grade from which the Asteromyzostomidae, Mesomyzostomatidae, and Protomyzostomidae arise (Lanterbecq et al. 2006). The Myzostomatidae clearly needs major revision, as does the genus *Myzostoma*.

The present analysis does not allow us to reconstruct without ambiguity the bodyplan of the organisms at the base of the myzostome clade. The ontogeny of myzostomes, however, suggests that the flat, discoidal shape of the trunk, the most common myzostome condition, and observed in many ectocommensals, is not the primitive condition. The discoidal shape of the trunk appears a few weeks af-

ter the larval metamorphosis, the trunk first being barrel shaped in juveniles (Eeckhaut & Jangoux 1993; Eeckhaut & Jangoux 1997).

Based on the integration of the phylogenetic, ontogenetic, and morphological data outlined here, we propose the following evolutionary scenario to explain the diversity of extant myzostome bodyplans. The first organisms to enter into an association with crinoids were segmented worms, probably with six body segments (Müller & Westheide 2000) and five pairs of polychaete-type parapodia (Bleidorn et al. 2007; Lanterbecq et al. 2007) structured into cirrate neuro- and notopodia (Lanterbecq 2000; Michel 2004). As a result of adaptation to living on the crinoid body surface, which is most often curved (e.g., on the calyx, cirri, arms, and pinnules), the notopodia of these organisms disappeared and the neuropodia migrated ventrally, allowing them to anchor more firmly or/and to move more efficiently on the crinoids (Lanterbecq et al. 2007). Clade 1 has the ancestral condition of being a dimorphic parasitic form probably living in a gall (Lanterbecq et al. 2006). Because such parasites spent most of their life walled up, sensory organs (i.e., the supposedly

chemosensory lateral organs and the putatively mechanosensory marginal cirri) became reduced or totally disappeared in both the females and the dwarf males. Both sexes retained some capability for movement, but their parapodia were highly reduced. Males mainly served for the transfer of spermatozoa, and females developed principally to function as brooders of ova. The female trunk thus became somewhat hypertrophied, and the expanding ventral side tended to push the parapodial vestiges dorsally.

The ancestral condition for clade 2 of being monomorphic with an introvert, a discoidal trunk, ten pairs of needle-shaped cirri, and strong parapodia appears to be coincident with moving freely over the host crinoid's body surface. From this, three main morphotypes were derived that can still be observed in the extant myzostome fauna: those of typical species of *Myzostoma*, *Hypomyzostoma*, and *Mesomyzostoma*. Most of the *Myzostoma*-type species are highly mobile (Lanterbecq et al. 2007) and they are able to move quickly over the host crinoids; furthermore, they often mimic the colors and color patterns of their hosts (Grygier 2000). Several times, the *Myzostoma*-type myzostomes have given rise to parasitic forms with consequent changes in anatomy (Lanterbecq et al. 2006). A large number of somewhat sessile (ectoparasites fixed to the host), thick-bodied, or dome-like species that are currently classified in *Myzostoma* (e.g., *Myzostoma glabrum*), as well as *Contramyzostoma*, *Notopharyngoides*, and *Asteromyzostomum* species, are examples of such parasites. Most show a reduction of their locomotory appendages and sensory organs, and others present massive parapodia whose locomotory ability is reduced, but present an advantage in anchorage to the host.

The *Hypomyzostoma*-type myzostomes (exemplified by *Hypomyzostoma* spp., *Myzostoma fissum*, *Myzostoma furcatum*, and *Myzostoma laingense*) have well-developed mimicry. Their body is thick and they do not move quickly over the crinoid surface, but mainly remain attached to pinnules or the aboral sides of the arms. Some of them (e.g., *M. furcatum*) have developed caudal appendages and dorsal ridges that appear to mimic crinoid pinnules; they also show striking similarities to their host's color pattern. To live on the arms, *Hypomyzostoma*-type myzostomes have become elongate and many have developed transverse ridges similar to arm ossicles. From the elongated myzostomes of this kind the parasitic *Mesomyzostoma*-type species were derived, including representatives of *Mesomyzostoma* and *Protomyzostomum* (Lanterbecq et al. 2006), which parasitize the coelom and gonads of crinoids and ophiuroids, respectively. They are cylindrical and in-

sert themselves into the coelomic sinuses and in the gonads. They do not have obvious sensory organs and their parapodia are reduced to only the chaetae.

Ghiselin (1969) proposed that hermaphroditism evolves in groups (i) in which it is hard to find a mate; (ii) in which one sex benefits from being larger or smaller than the other; or (iii) in which there are small, genetically isolated populations. Finding a mate may have been the principal driving factor in the origin of hermaphroditism in this clade of myzostomes, considering that they are all obligate symbionts of echinoderms, and that conspecifics must be sexually mature at the same time and must live on the same host individual, often at low densities. Moreover, the only known method of reproduction in myzostomes is the hypodermic transfer of spermatozoa from one individual to another (Eeckhaut & Jangoux 1991; Eeckhaut 1995), which implies that physical contact is necessary between mates. We observe a basal split between simultaneous hermaphroditism and gonochorism, but the ancestral condition for myzostomes cannot be resolved with confidence in our present analyses. Resolution of the sister group of Myzostomida may allow for a better inference of the origin of hermaphroditism in the group. Gonochorism is present in myzostomes when the female stage is non-motile, enclosed in galls or cysts. A gallicolous or a cysticolous life style is certainly advantageous in terms of being better protected against predators, but it drastically reduces the opportunity for mate contacts. The driving force favoring gonochorism in myzostomes has probably been the non-motility of individuals.

The anatomy of parasites may be drastically modified with respect to the free-living organisms from which they evolved. Some appendages and/or internal organs undergo development while others are reduced or totally disappear. A good example of the elaboration of appendages is in Platyhelminthes, where anchorage devices in Monogenea, Digenea, and Cestoda are often very elaborate. Myzostomes also illustrate what may occur during the evolution of organisms with a wide range of symbiotic lifestyles. Here, the locomotory (parapodia) and sensory organs (lateral organs and cirri) have regressed or hypertrophied multiple times independently, in parallel with the emergence of particular lifestyles. The main factor that has led to the extant myzostome bodyplans appears to be the crinoid body part that is infested: myzostomes became (i) threadlike in coelomic parasites, (ii) bean-shaped in gallicolous parasites, digestive-system parasites, and most cysticolous parasites, (iii) flat and discoidal in most ectocommensals and in ectoparasites, or (iv) thick and resembling cer-

tain crinoid appendages in other ectocommensals. Although the degree of host specificity of myzostomes is quite variable among species (Grygier 1990, 2000), we expect that further investigation of the phylogeny of crinoids and myzostomes will reveal that cospeciation events have played a major role in the life history of Myzostomida.

Acknowledgments. The National Fund for Scientific Research, Belgium (FRFC contract numbers 2.4.567.04.F and 2.4583.05), provided substantial support for this work. Déborah Lanterbecq was supported by a PhD grant from the “Fonds pour la formation à la recherche dans l’industrie et dans l’agriculture” (FRIA) and is now supported by a Postdoctoral Research Associate grant from the “Fonds de la recherche scientifique” (FNRS). The authors thank the two reviewers for their helpful comments on the manuscript.

References

- Bleidorn C, Eeckhaut I, Podsiadlowski L, Schult N, McHugh D, Halanych KM, Milinkovitch MC, & Tiedemann R 2007. Mitochondrial genome and nuclear sequence data support Myzostomida as part of the annelid radiation. *Mol. Biol. Evol.* 24: 1690–1701.
- Brett CE 1978. Host-specific pit-forming epizoans on Silurian crinoids. *Lethaia* 11: 217–232.
- Cunningham CW, Omland KE, & Oakley TH 1998. Reconstructing ancestral character states: a critical reappraisal. *Trends Ecol. Evol.* 13: 361–366.
- Crisp MD & Cook LG 2005. Do early branching lineages signify ancestral traits? *Trends Ecol. Evol.* 20: 122–128.
- Eeckhaut I 1995. Cycle vital et biologie de *Myzostoma cirriferum* (Myzostomida), symbioteobligatoire de la comatule *Antedon bifida* (Echinodermata). PhD dissertation, University of Mons-Hainaut, Mons, Belgium. 106 pp.
- 1998. *Mycomyzostoma calcidicola* gen. nov., sp. nov., the first extant parasitic myzostome infesting crinoid stalks, with a nomenclatural appendix by M.J. Grygier. *Species Divers.* 3: 89–103.
- Eeckhaut I & Jangoux M 1991. Fine structure of the spermatophore and intradermic penetration of sperm cells in *Myzostoma cirriferum* (Annelida, Myzostomida). *Zoomorphology* 111: 49–58.
- 1992. Development and behaviour of *Myzostoma alatum* and *Pulvinomyzostomum pulvinar*, two myzostomids symbiotes of the comatulid *Leptometra phalangium* (Echinodermata). In: Echinoderm Research 1991. Scaleira-Liaci L & Canicatti C, eds., pp. 229–236. Balkema, Rotterdam, the Netherlands.
- 1993. Life cycle and mode of infestation of *Myzostoma cirriferum* (Annelida), a symbiotic myzostomid of the comatulid crinoid *Antedon bifida* (Echinodermata). *Dis. Aqat. Org.* 15: 207–217.
- 1995. *Contramyzostoma bialatum* (Annelida: Myzostomida), a new genus and species of parasitic myzostome infesting comatulid crinoids. *Raffles Bull. Zool.* 43: 343–353.
- 1997. Infestation, population dynamics, growth and reproductive cycle of *Myzostoma cirriferum* (Myzostomida), an obligate symbiont of the comatulid crinoid *Antedon bifida* (Crinoidea, Echinodermata). *Cah. Biol. Mar.* 38: 7–18.
- Eeckhaut I, Grygier MJ, & Deheyn D 1998. Myzostomes from Papua New Guinea, with related Indo-West Pacific distribution records and description of five new species. *Bull. Mar. Sci.* 62: 841–886.
- Eeckhaut I, McHugh D, Mardulyn P, Tiedemann R, Monteyne D, Jangoux M, & Milinkovitch MC 2000. Myzostomida: a link between trochozoans and flatworms? *Proc. R. Soc. Lond. B* 267: 1–10.
- Eeckhaut I & Lanterbecq D 2005. Myzostomida: a review of their ultrastructure and phylogeny. In: *Morphology, Molecules and Evolution of the Polychaeta and Related Taxa*. Bartholomaeus T & Purschke G, eds. *Hydrobiologia* 535/536: 253–275.
- Fitzhugh K 2006. The ‘requirement of total evidence’ and its role in phylogenetic systematics. *Biol. Philos.* 21: 309–351.
- Ghiselin MT 1969. The evolution of hermaphroditism among animals. *Q. Rev. Biol.* 44: 189–208.
- Graff Lv 1884. Report on the Myzostomida collected during the voyage of H.M.S. Challenger during the years 1873–76. *Rep. Scient. Res. Voy. H.M.S. Challenger 1873–1876*, Zool. 10: 1–82, plates I–XVI.
- Grygier MJ 1990. Distribution of Indo-Pacific *Myzostoma* and host specificity of comatulid-associated Myzostomida. *Bull. Mar. Sci.* 47: 182–191.
- 1992. Hong Kong Myzostomida and their Indo-Pacific distributions. In *The Marine Flora and Fauna of Hong Kong and Southern China, III*. Proceedings of the 4th International Marine Biological Workshop. Morton B, ed., pp. 131–147. Hong Kong University Press, Hong Kong.
- 2000. Class Myzostomida. In: *Polychaetes and Allies: The Southern Synthesis. Fauna of Australia, Vol. 4A Polychaeta, Myzostomida, Pogonophora, Echiura, Sipuncula*. Beesley PL, Ross GJB, & Glasby CJ, eds., pp. 297–330. CSIRO Publishing, Melbourne, Australia.
- Jägersten G 1940. Zur Kenntnis der Morphologie, Entwicklung und Taxonomie der Myzostomida. *Nova Acta R. Soc. Sci. Upsal.* 11: 1–84.
- Lanterbecq D 2000. Phylogénèse et évolution des plans de structure chez les myzostomides (Spiralia: Myzostomida). Master thesis, University of Mons-Hainaut, Mons, Belgium. 48 pp.
- Lanterbecq D, Rouse GW, Milinkovitch MC, & Eeckhaut I 2006. Multiple DNA data sets suggest independent emergence of parasites in the Myzostomida (Protostomia). *Syst. Biol.* 55: 208–227.
- Lanterbecq D, Bleidorn C, Michel S, & Eeckhaut I 2007. Locomotion and fine structure of parapodia in *Myzo-*

- stoma cirriferum* (Myzostomida). Zoomorphology 127: 59–68.
- Lemmon AR & Milinkovitch MC 2002. MetaPIGA (Phylogeny inference using the MetaGA) version 1.0.2b. Distributed by the authors. Available at <http://www.lanevol.org/LANE/Welcome.html>
- Lewis PO 2001. A likelihood approach to estimating phylogeny from discrete morphological character data. Syst. Biol. 50: 913–925.
- Maddison WP & Maddison DR 2000. MacClade Version 4.0. Sinauer, Sunderland, MA, USA.
- 2004. Mesquite: a modular system for evolutionary analysis. Version 1.01. Available at <http://mesquiteproject.org>
- Marotta R, Ferraguti M, Erséus C, & Gustavsson LM 2008. Combined-data phylogenetics and character evolution of Clitellata (Annelida) using 18S rDNA and morphology. Zool. J. Linn. Soc. Lond. 154: 1–26.
- Meyer DL & Ausich WI 1983. Biotic interactions among recent and among fossil crinoids. In: Biotic Interactions in Recent and Fossil Benthic Communities. Tevesz MJS & McGall PL, eds., pp. 377–427. Plenum Press, New York, NY, USA.
- Michel S 2004. Locomotion et structure des parapodes chez *Myzostoma cirriferum* (Myzostomida). Master thesis, University of Mons-Hainaut, Mons, Belgium. 37 pp.
- Müller MC & Westheide W 2000. Structure of the nervous system of *Myzostoma cirriferum* (Annelida) as revealed by immunohistochemistry and cLSM analyses. J. Morphol. 245: 87–98.
- Omland KE 1999. The assumptions and challenges of ancestral state reconstructions. Syst. Biol. 48: 604–611.
- de Queiroz K 1996. Including the characters of interest during tree reconstruction and the problems of circularity and bias in studied of character evolution. Am. Nat. 148: 700–708.
- Radwanska U & Radwanski A 2005. Myzostomid and copepod infestation of Jurassic echinoderms: a general approach, some new occurrences, and/or re-interpretation of previous reports. Acta Geol. Pol. 55: 109–130.
- Ronquist F 2004. Bayesian inference of character evolution. Trends Ecol. Evol. 19: 475–481.
- Ronquist F & Huelsenbeck JP 2003. MRBAYES 3: Bayesian phylogenetic inference under mixed models. Bioinformatics 19: 1572–1574.
- Rouse GW & Fauchald K 1997. Cladistics and polychaetes. Zool. Scr. 26: 139–204.
- Swofford D 1998. PAUP*: Phylogenetic Analysis Using Parsimony (* and other methods). Beta version 4.0.b1. Sinauer, Sunderland, MA, USA.
- Warn JM 1974. Presumed myzostomid infestation of an ordovician crinoid. J. Paleontol. 48: 506–513.

Appendix 1

Vouchers of the new species (and some others) are deposited at the South Australian Museum (SAM) or at the Belgian Royal Institute for Natural Sciences (IRSNB).

Host abbreviations: CC = comatulid crinoid, SC = stalked crinoid. Ectocommensals move around on the external surface of crinoids; some stay on the crinoid calyx and divert food particles from the host's ambulacral grooves; other stay preferably on the pinnules or the arms. Ectoparasites are externally fixed by their chaetae on the calyx of the crinoid, close to the host's mouth, from which they steal food particles. Endoparasites can be located in the anterior part of the digestive system, in the gonads, or in the integument (where they form galls or cysts). Cysticolous parasites live in a soft and uncalcified cyst located on the crinoid host's arm or mouth. Gallicolous parasites induce galls on arms by deformation of the original crinoid's ossicles.

The characters and their states are explained in detail in the text; in summary:

1. Dimorphism versus monomorphism: (0) dimorphic; (1) monomorphic; (?) data missing or unavailable.
2. Gonochorism versus hermaphroditism: (0) gonochoric; (1) simultaneously hermaphroditic; (?) data missing or unavailable.
3. Trunk shape: (0) $L \approx W$; (1) $W > L$; (2) $L > W$.
4. Trunk curvature: (0) convexo-concave; (1) concavo-convex; (2) convexo-convex.
5. Number of marginal cirri: (0) >20 (ten pairs); (1) $=20$; (2) absent; (3) <20 .
6. Shape of marginal cirri: (0) tooth; (1) hump; (2) needle; (3) club; (4) absent.
7. Length of marginal cirri: (0) equal; (1) not equal; (2) absent.
8. Number of lateral organs: (0) absent; (1) 4 pairs; (2) >4 pairs.
9. Parapodia: (0) type 1; (1) type 2; (2) type 3.
10. Parapodial cirrus: (0) absent; (1) present.
11. Body surface (ciliature): (0) sparse; (1) dense.
12. Introvert: (0) absent; (1) present.
13. Dorsal ridges: (0) absent; (1) present.
14. Caudal appendages: (0) absent; (1) present.

Appendix 1. List of taxa examined in this study, along with their lifestyle, host type, and states of the 14 adult characters

Species	Lifestyle	Host	Character numbers													
			1	2	3	4	5	6	7	8	9	10	11	12	13	14
<i>Myzostoma toliarense</i> LANTERBECQ & EECKHAUT 2003	Cysticolous parasite	CC	1	1	1	1	0	2	1	1	0	0	0	1	0	0
<i>Myzostoma pseudocuniculus</i> LANTERBECQ & EECKHAUT 2003	Ectocommensal (on pinnules)	CC	1	1	2	0	0	2	1	1	0	0	0	1	0	1
<i>Myzostoma cuniculus</i> EECKHAUT, GRYGIER, & DEHEYN 1998	Ectocommensal (on pinnules)	CC	1	1	2	0	1	2	0	1	0	0	0	1	0	1
<i>Myzostoma nigromaculatum</i> EECKHAUT, GRYGIER, & DEHEYN 1998	Ectocommensal (on calyx)	CC	1	1	0	0	1	2	1	1	0	0	0	1	0	0
<i>Myzostoma ambiguum</i> GRAFF 1887	Ectocommensal (on calyx)	CC	1	1	2	0	1	2	1	1	0	0	0	1	0	0
<i>Myzostoma capitocutis</i> EECKHAUT, VANDENSPIEGEL, & GRYGIER 1994	Ectocommensal (on calyx)	CC	1	1	0	0	0	2	1	1	0	0	0	1	0	0
<i>Myzostoma fissum</i> GRAFF 1884	Ectocommensal (on pinnules)	CC	1	1	2	0	1	0	1	1	0	1	0	1	1	1
<i>Myzostoma mortenseni</i> JÄGERSTEN 1940	Ectocommensal (on calyx)	CC	1	1	0	0	0	3	1	1	0	1	0	1	0	0
<i>Myzostoma glabrum</i> LEUCKART 1842	Ectoparasite (fixed on calyx)	CC														
	Female		1	0	0	0	1	1	0	1	0	0	0	1	0	0
	Male		1	0	0	0	1	1	0	1	0	0	0	1	0	0
<i>Myzostoma alatum</i> GRAFF 1884	Ectoparasite (fixed on calyx)	CC														
	Female		1	0	0	0	1	1	0	1	0	0	0	1	0	0
	Male		1	0	0	0	1	1	0	1	0	0	0	1	0	0
<i>Myzostoma cirriferum</i> LEUCKART 1827	Ectocommensal (on calyx)	CC	1	1	0	0	1	2	0	1	0	0	0	1	0	0
<i>Myzostoma polycyclus</i> ATKINS 1927	Ectocommensal (on calyx)	CC	1	1	0	0	0	2	1	1	0	1	0	1	0	0
<i>Myzostoma laingense</i> EECKHAUT, GRYGIER, & DEHEYN 1998	Ectocommensal (on pinnules)	CC	1	1	2	0	0	1	1	1	0	1	0	1	1	1
<i>Myzostoma furcatum</i> GRAFF 1887	Ectocommensal (on pinnules)	CC	1	1	2	0	0	0	1	1	0	1	0	1	1	1
<i>Myzostoma coriaceum</i> GRAFF 1884	Ectocommensal (on calyx)	CC	1	1	0	0	1	2	0	1	0	0	0	1	0	0
<i>Notopharyngoides aruensis</i> REMSCHEID 1918	Digestive system parasite	CC	1	1	2	1	2	4	2	1	0	0	1	1	0	0
<i>Hypomyzostoma fasciatum</i> REMSCHEID 1918	Ectocommensal (on arms)	CC	1	1	2	0	0	0	1	1	0	1	0	1	1	0
<i>Hypomyzostoma</i> sp. aff. <i>crosslandi</i> a BOULENGER 1913	Ectocommensal (on arms)	CC	1	1	2	0	0	0	0	1	0	1	0	1	0	0
<i>Hypomyzostoma</i> sp. aff. <i>crosslandi</i> b BOULENGER 1913	Ectocommensal (on arms)	CC	1	1	2	0	0	0	0	1	0	1	0	1	0	0
<i>Hypomyzostoma</i> n. sp.1 (SAM)	Ectocommensal (on arms)	CC	1	1	2	0	0	0	1	1	0	1	0	1	1	0
<i>Pulvinomyzostomum pulvinar</i> GRAFF 1884	Digestive system parasite	CC														
	Female		0	0	1	1	2	4	2	2	1	0	1	0	0	0
	Male		0	0	2	0	2	4	2	2	1	0	1	0	0	0
<i>Contramyzostoma sphaera</i> EECKHAUT, GRYGIER, & DEHEYN 1998	Cysticolous parasite	CC	1	1	1	1	1	2	0	1	1	0	0	1	0	0

Appendix 1. (cont'd).

Species	Lifestyle	Host	Character numbers													
			1	2	3	4	5	6	7	8	9	10	11	12	13	14
<i>Endomyzostoma clarki</i> MCLENDON 1906	Gallicolous parasite	SC														
	Female		0	0	2	1	3	2	0	1	1	0	0	0	0	0
	Male		0	0	0	0	3	2	0	1	1	0	0	0	0	0
<i>Endomyzostoma tenuispinum</i> GRAFF 1884	Gallicolous parasite	SC														
	Female		0	0	2	1	3	2	0	1	1	0	0	0	0	0
	Male		0	0	0	0	3	2	0	0	1	0	0	0	0	0
<i>Endomyzostoma deformatior</i> GRAFF 1884	Gallicolous parasite	SC	1	1	0	1	2	4	2	0	1	0	0	0	0	0
<i>Endomyzostoma cysticum</i> GRAFF 1883	Cysticolous parasite	CC														
	Female		0	0	2	1	2	4	2	0	1	0	0	0	0	0
	Male		0	0	0	1	2	4	2	0	1	0	0	0	0	0
<i>Endomyzostoma</i> n. sp. 1 IRSNB	Cysticolous parasite	CC	?	?	2	1	2	4	2	0	1	0	0	0	0	0
<i>Endomyzostoma</i> n. sp. 2 (SAM)	Gallicolous parasite	SC	?	?	2	1	2	4	2	0	1	0	0	0	0	0
<i>Endomyzostoma</i> n. sp. 3 (SAM)	Ectocommensal	SC	?	?	0	0	1	2	1	0	1	0	0	0	0	0
<i>Mesomyzostoma</i> n. sp. 2 (SAM)	Gonads parasite	CC	1	1	2	1	2	4	2	2	2	0	1	0	0	0
<i>Mesomyzostoma katoi</i> OKADA 1933	Gonads parasite	CC	1	1	2	1	2	4	2	2	2	0	1	0	0	0
<i>Mesomyzostoma</i> n. sp. 4b (SAM)	Gonads parasite	CC	1	1	2	1	2	4	2	0	2	0	1	0	0	0
<i>Mesomyzostoma</i> n. sp. 3a (SAM)	Gonads parasite	CC	1	1	2	2	2	4	2	0	2	0	1	0	0	0
<i>Mesomyzostoma</i> n. sp. 3b (SAM)	Gonads parasite	CC	1	1	2	2	2	4	2	0	2	0	1	0	0	0
<i>Mesomyzostoma reichenspergi</i> REMSCHIED 1918	Gonads parasite	CC	1	1	2	1	2	4	2	0	2	0	1	0	0	0
<i>Mesomyzostoma</i> n. sp. 4a (SAM)	Gonads parasite	CC	1	1	2	1	2	4	2	0	2	0	1	0	0	0
<i>Mesomyzostoma</i> n. sp. 1a (SAM)	Gonads parasite	CC	1	1	2	1	2	4	2	0	2	0	1	0	0	0
<i>Mesomyzostoma</i> n. sp. 1b (SAM)	Gonads parasite	CC	1	1	2	1	2	4	2	0	2	0	1	0	0	0